Electric field effects on hot and dense media

Osvaldo Ferreira

UFRJ
UNIVERSIDADE FEDERAL
DO RIO DE JANEIRO

60th International School for
Subnuclear Physics
Erice, 2024

Motivation

The QCD phase diagram in background fields

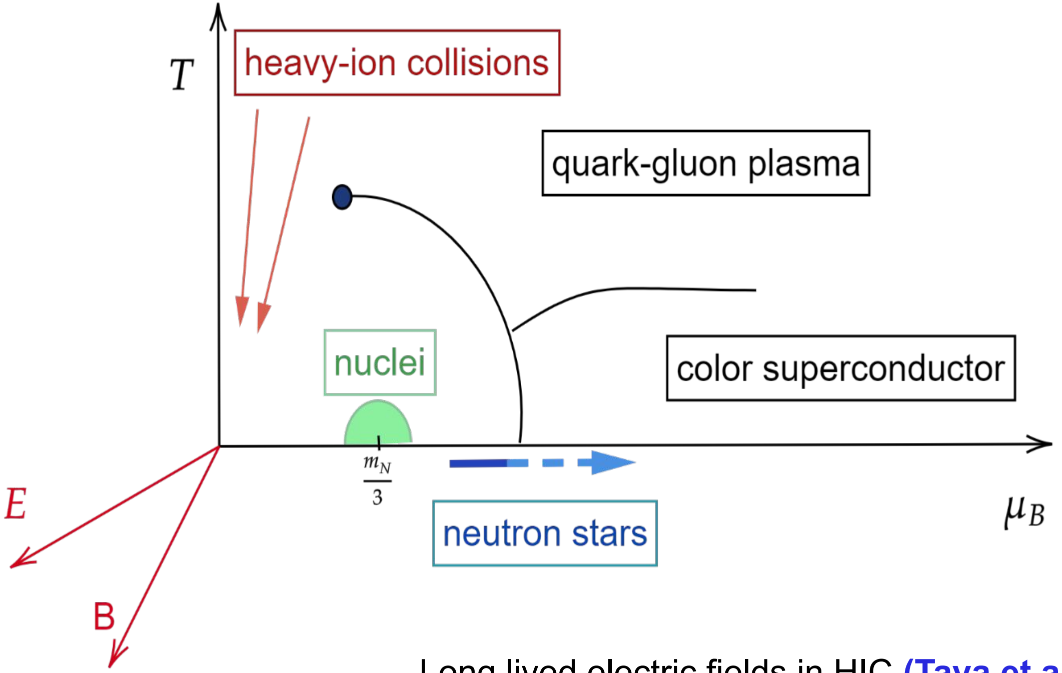

Long lived electric fields in HIC **(Taya et al, arxiv, 2024)**

Neutron stars

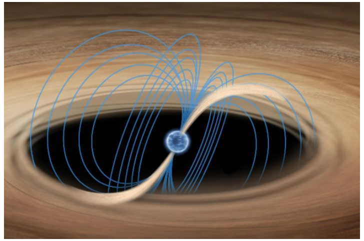

Heavy-ions collisions

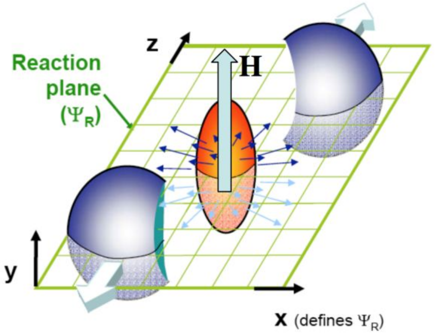

(Kharzeev, PPNP, 2014)

Motivation

The QCD phase diagram in background fields

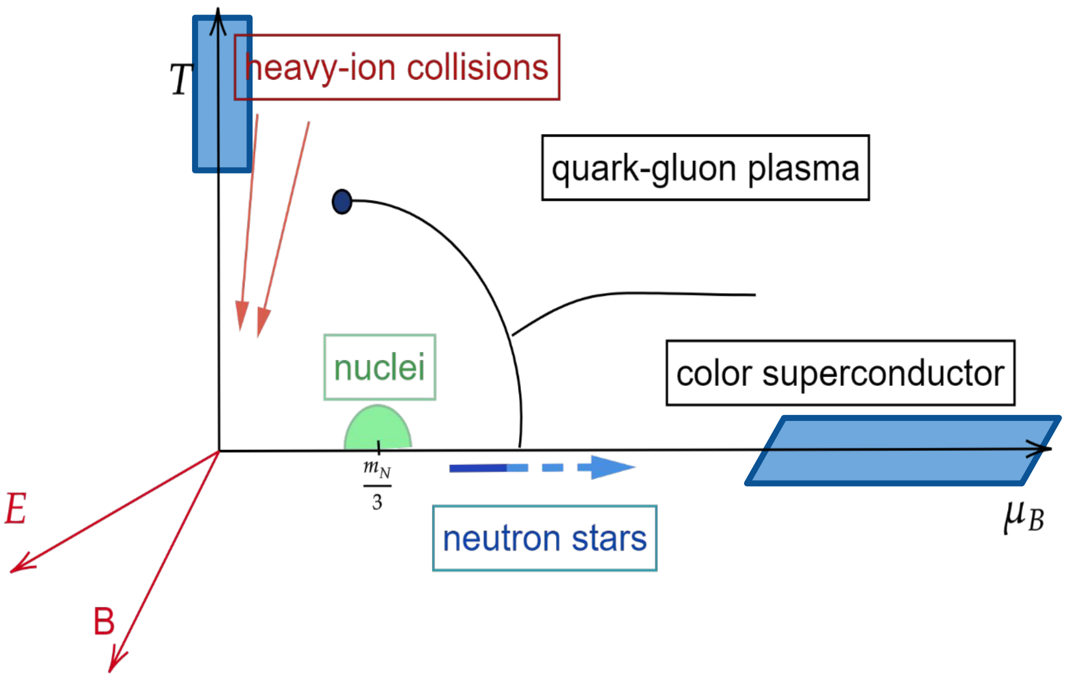

In this work we look at linear responses in the limit of high temperatures or high densities

The electromagnetic susceptibilities

The electromagnetic susceptibilities are the linear response of a system to the application of external **electric** and magnetic fields.

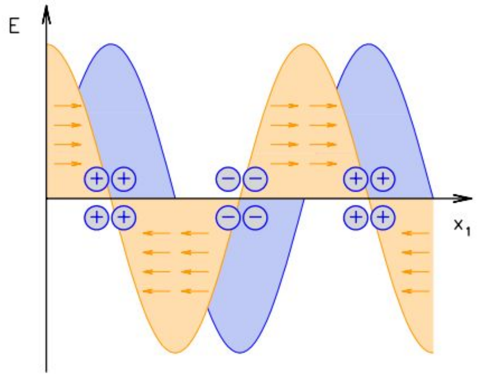

(Endrődi and Markó, JHEP, 2022)

Equilibrium: the electric field induces a charge distribution in the medium which in turn balances the electric force of the external field. **Here: Fermi pressure vs electric force**

The electromagnetic susceptibilities: two approaches

1) **Free energy for constant EM fields**

Schwinger: $\Omega(E, B) =$ 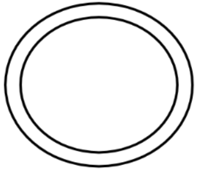

(Lowe and Rojas, PRD, 1992)

(Elmfors and Skagerstam,Phys.Lett.B, 1995)

(Gies, PRD, 1995)

2) **Expand for weak fields**

$$\Omega = \xi \frac{E^2}{2} + \chi \frac{B^2}{2} + O\left(E^4,\ B^4,\ E^2 B^2\right)$$

Adapted from Endrődi's talk at EESIM, 2022

The electromagnetic susceptibilities: two approaches

1) Free energy for constant EM fields

2) Expand for weak fields

Schwinger: $\Omega(E, B) =$ 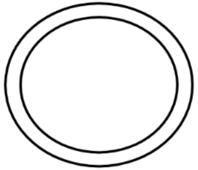

$$\Omega = \xi \frac{E^2}{2} + \chi \frac{B^2}{2} + O\left(E^4,\ B^4,\ E^2 B^2\right)$$

Expand the free energy in terms of the background fields from the start

Weldon: $\Omega(A) =$ 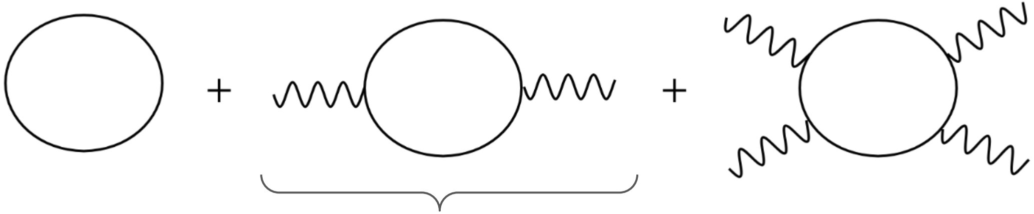 $+ \ O\left(A^6\right)$

(Weldon, PRD, 1982)

$\xi,\ \chi \sim \Pi_{\mu\nu}$ → Photon polarization tensor

Adapted from Endrődi's talk at EESIM, 2022

Disagreement with Schwinger's method

In **(Endrődi and Markó, JHEP, 2022)** the susceptibilities are computed using a High-temperature expansion within the real-time formalism.

$$\xi_{Weldon} - \xi_{Schwinger} = -\frac{1}{6\pi^2} + \mathcal{O}\left(\frac{m^2}{T^2}\right)$$

The $\underbrace{\text{magnetic susceptibilities}}_{\chi}$ agree, but the electric ones do not.

The electromagnetic susceptibilities in Weldon's approach

(Endrődi and Markó, JHEP, 2022)

Equilibrium distribution

$$\xi = \frac{1}{e^2} \lim_{k\to 0} \lim_{k_0\to 0} \left[\frac{\Pi_{00}^{T\neq 0}(k_0,k) - \Pi_{00}^{T\neq 0}(0,0)}{k^2} \right]$$

$$= \frac{1}{2e^2} \lim_{k\to 0} \lim_{k_0\to 0} \frac{\partial^2 \Pi_{00}^{T\neq 0}(k_0,k)}{\partial k^2}$$

(Electric)

Vacuum term removed (T=0)

$$\chi = \frac{1}{2e^2} \lim_{k\to 0} \lim_{k_0\to 0} \frac{\partial^2 \Pi_{S}^{T\neq 0}(k_0,k)}{\partial k^2}$$

(Magnetic)

The electromagnetic susceptibilities: early lattice results

(Endrődi and Markó, PRD, 2022)

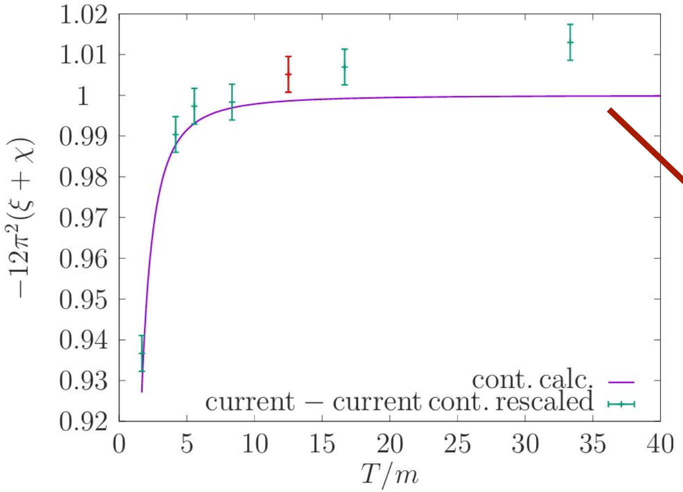

$$\xi = -\frac{1}{12\pi^2}\left(\log\frac{T^2\pi^2}{m^2} - 2\gamma_E + 1\right) + \frac{31\zeta'(-4)}{192\pi^2}\frac{m^4}{T^4} + \mathcal{O}\left(\frac{m^6}{T^6}\right)$$

$$\chi = \frac{1}{12\pi^2}\left(\log\frac{T^2\pi^2}{m^2} - 2\gamma_E\right) - \frac{7\zeta'(-2)}{12\pi^2}\frac{m^2}{T^2} + \mathcal{O}\left(\frac{m^4}{T^4}\right)$$

$$\xi + \chi = -\frac{1}{12\pi^2} - \frac{7\zeta'(-2)}{12\pi^2}\frac{m^2}{T^2} + \mathcal{O}\left(\frac{m^4}{T^4}\right)$$

The dots are the results obtained on the Lattice.

Only mass corrections appear in the sum.

From now on, all expressions are from Weldon's approach on.

Electromagnetic susceptibilities and power corrections

$$\xi = \frac{1}{2e^2} \lim_{k\to 0} \lim_{k_0 \to 0} \frac{\partial^2 \Pi_{00}^{T\neq 0}(k_0, k)}{\partial k^2}$$

→ The susceptibilities are associated to power corrections to the photon polarization tensor.

We applied the methods of **(Gorda et al, PRD, 2023):** real-time formalism for QFT at finite temperature and density

Alternative calculations for power corrections: **(Carignano et al,Phys.Lett.B, 2018), (Manuel et al, PRD, 2016).**

Hard thermal loop expansion should in principle lead to the same results as high-temperature expansion.

The electromagnetic susceptibilities

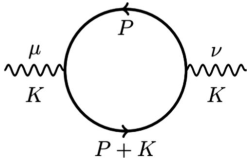

$$\Pi^{\mu\nu}(K) = \mathcal{P}^{\mu\nu}_{\mathrm{T}}(K)\Pi_{\mathrm{T}}(K) + \mathcal{P}^{\mu\nu}_{\mathrm{L}}(K)\Pi_{\mathrm{L}}(K)$$

Keep the vacuum the term

$$\chi = -\frac{1}{2e^2} \lim_{k\to 0} \lim_{k_0\to 0} \frac{\partial^2 \Pi_{\mathrm{T}}(k_0, k)}{\partial k^2},$$

$$\xi = \frac{1}{2e^2} \lim_{k\to 0} \lim_{k_0\to 0} \frac{\partial^2 \Pi_{\mathrm{L}}(k_0, k)}{\partial k^2},$$

(OF and Eduardo S. Fraga, PRD, 2024)

The photon polarization tensor

The power and mass corrections

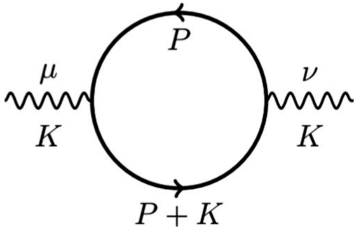

$$\Pi_{\rm L} = \frac{-K^2}{k^2}\Pi_{00} \quad , \quad \Pi_{\rm T} = \frac{1}{d-1}\left(\Pi^{\mu}_{\mu} + \frac{K^2}{k^2}\Pi_{00}\right)$$

$$\Pi^R_{00}(K) = 4e^2 \int_P \Delta^d(P)\left[N_F^-(P) + N_F^+(P)\right]\frac{2p_0^2 + 2k^0p^0 + K\cdot P}{2K\cdot P + K^2},$$

$$(\Pi^R)^{\mu}_{\mu} = -4e^2 \int_P \Delta^d(P)\left[N_F^-(P) + N_F^+(P)\right]\left[\frac{(D-2)K\cdot P + 2m^2}{K^2 + K\cdot P}\right]$$

$K \ll P$ and $m \ll T,\ \mu \sim P$

1) Expand to obtain the power corrections

2) Expand for small masses around the massless solution

Results for the susceptibilities

The high-temperature limit

$$\xi = -\frac{1}{12\pi^2}\left(\ln\frac{T^2\pi^2}{\bar{\Lambda}^2} - 2\gamma_E + 1\right) - \frac{31\zeta'(-4)}{192\pi^2}\frac{m^4}{T^4} + \mathcal{O}\left(\frac{m^6}{T^6}\right),$$

$$\chi = \frac{1}{12\pi^2}\left(\ln\frac{T^2\pi^2}{\bar{\Lambda}^2} - 2\gamma_E\right) - \frac{7\zeta'(-2)}{12\pi^2}\frac{m^2}{T^2} + \mathcal{O}\left(\frac{m^4}{T^4}\right)$$

- Negative electric susceptibilities and positive magnetic susceptibilities (paramagnet) which agrees with **(Endrődi and Markó, PRD, 2022) (Bali et al, JHEP,2020).**
- Electric susceptibilities also disagree with the result from the Schwinger's method.
- Both a renormalization scale and a mass appear in our results.

Results for the susceptibilities

The high-temperature limit

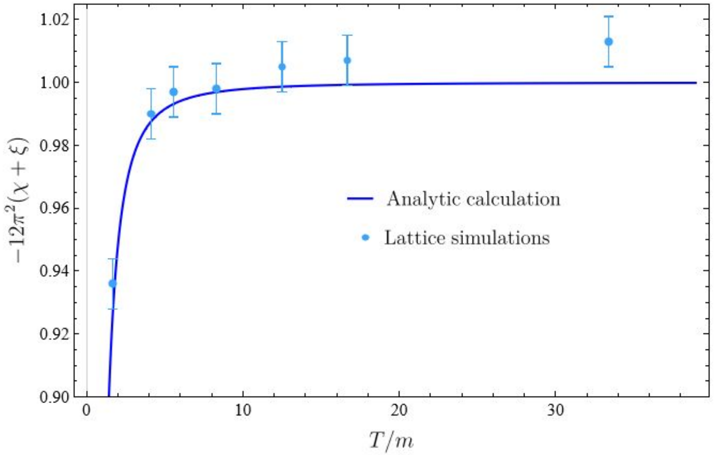

$$\xi + \chi = -\frac{1}{12\pi^2} - \frac{7\zeta'(-2)}{12\pi^2}\frac{m^2}{T^2} + \mathcal{O}\left(\frac{m^4}{T^4}\right),$$

(Endrődi and Markó, PRD, 2024)

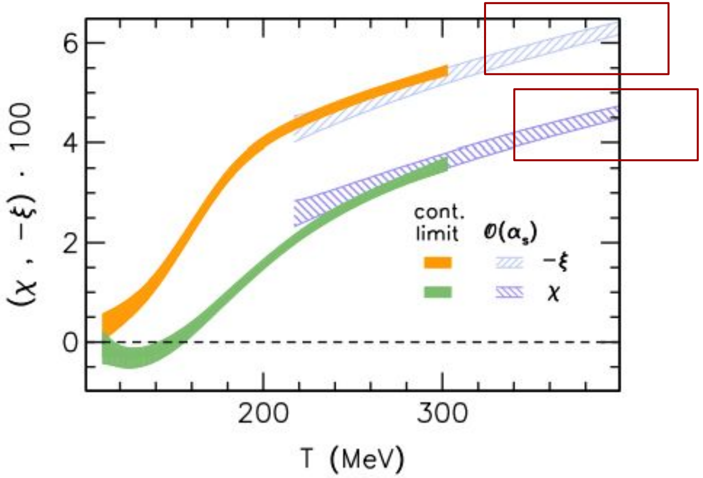

$$\xi = -\frac{1}{12\pi^2}\left(\ln\frac{T^2\pi^2}{\bar{\Lambda}^2} - 2\gamma_E + 1\right)$$

$$\chi = \frac{1}{12\pi^2}\left(\ln\frac{T^2\pi^2}{\bar{\Lambda}^2} - 2\gamma_E\right)$$

Conclusions and perspectives

In this work

- We have shown how the electric and magnetic susceptibilities can be computed using tools from hard thermal loop theory;
- Results for the high temperature limit agree well with lattice simulations and are consistent with m->0;
- We have extended previous results to the case of dense media.

For future work

- Interacting quarks within perturbative QCD (in progress);
- Extend the results for dense media to arbitrary masses.

Returning to the motivation...

- Still not clear why the Schwinger's method gives a different answer (ordering of limits?).

Backup slides

The photon polarization tensor

Results for the longitudinal component

$K \ll P$ *and* $m \ll T,\ \mu \sim P$

Mass corrections

$$\Pi_{\mathrm{L}}^{\mathrm{Pow}}(K) = \Pi_{\mathrm{L}}^{\mathrm{P0}} - K^2 \frac{e^2}{384\pi^2} \frac{m^4}{T^4} \left(\mathrm{Li}_{-4}^{(1)}(-e^{\frac{-\mu}{T}}) + \mathrm{Li}_{-4}^{(1)}(-e^{\frac{\mu}{T}}) \right) \left(1 + 8 \frac{k^2 k_0^2}{(K^2)^2} \right)$$

$$\Pi_{\mathrm{L}}^{\mathrm{P0}} = -\frac{e^2}{4\pi^2} \frac{2K^2}{3} \left\{ \ln \frac{2 \mathrm{e}^{-\gamma_{\mathrm{E}}} T}{\bar{\Lambda}} - 1 + \left(1 + \frac{K^2}{2k^2} \right) \left[1 - \frac{k^0}{2k} \ln \frac{k^0 + k + i\eta}{k^0 - k + i\eta} \right] - \mathrm{Li}_0^{(1)}\left(-\mathrm{e}^{\frac{\mu}{T}} \right) - \mathrm{Li}_0^{(1)}\left(-\mathrm{e}^{-\frac{\mu}{T}} \right) \right\} .$$

Do not contribute to the sum

For m-> 0 we recover the massless case **(Gorda et al, PRD, 2023), (Carignano et al,Phys.Lett.B, 2018), (Manuel et al, PRD, 2016).**

Results for the susceptibilities

The high-chemical potential limit

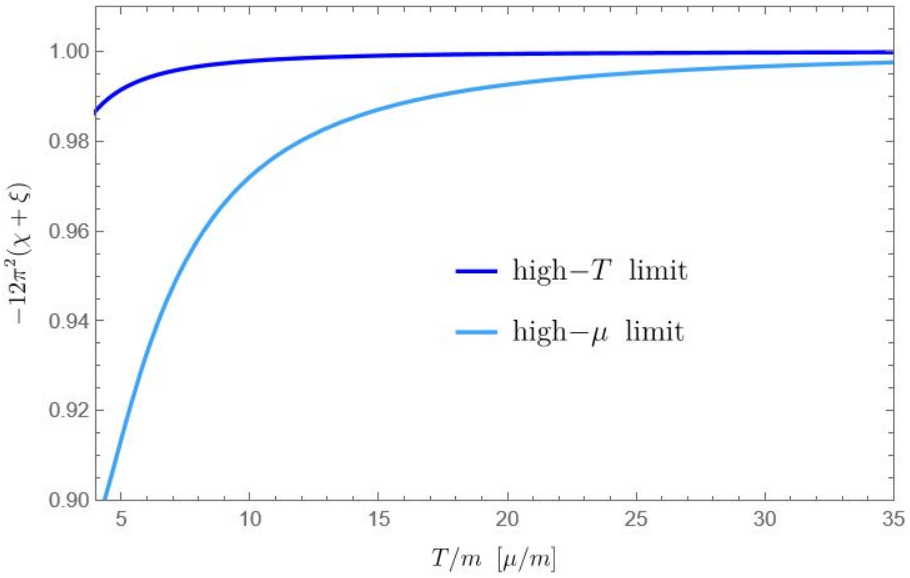

$$\chi + \xi = -\frac{1}{12\pi^2} + \frac{1}{6\pi^2}\frac{m^2}{\mu^2} + \mathcal{O}\left(\frac{m^4}{\mu^4}\right)$$

Similar qualitative behaviour, but the dense case reaches saturation more slowly.

Results for the susceptibilities

The high-chemical potential limit

$$\xi = -\frac{1}{12\pi^2}\left(\ln\frac{4\mu^2}{\bar{\Lambda}^2}+1\right)+\frac{1}{4\pi^2}\frac{m^4}{\mu^4}+\mathcal{O}\left(\frac{m^6}{\mu^6}\right),$$

$$\chi = \frac{1}{12\pi^2}\left(\ln\frac{4\mu^2}{\bar{\Lambda}^2}\right)+\frac{1}{6\pi^2}\frac{m^2}{\mu^2}+\mathcal{O}\left(\frac{m^4}{\mu^4}\right)$$

The signs for the susceptibilities are the same as in the high-temperature limit: negative electric susceptibilities and positive magnetic susceptibilities.

Susceptibilities without equilibrium requirement: more complications

(Endrődi and Markó, JHEP, 2022)

Equilibrium distribution

$$\xi = \frac{1}{e^2} \lim_{k\to 0} \lim_{k_0\to 0} \left[\frac{\Pi_{00}^{T\neq 0}(k_0,k) - \Pi_{00}^{T\neq 0}(0,0)}{k^2} \right]$$

$$\xi_{\mathrm{Weldon}}^{\mathrm{non-equi}} = \frac{T^2}{3k_1^2} + \mathcal{O}(k_1^0)$$

Taking the k-> 0 limit leads to a divergence

The photon polarization tensor

The power and mass corrections

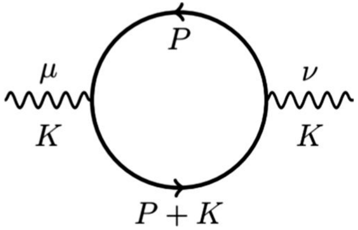

$$\Pi_{\mathrm{L}} = \frac{-K^2}{k^2}\Pi_{00} \quad , \quad \Pi_{\mathrm{T}} = \frac{1}{d-1}\left(\Pi^{\mu}_{\mu} + \frac{K^2}{k^2}\Pi_{00}\right)$$

$K \ll P$

$$\Pi^{\mathrm{Pow}}_{00}(K) = \frac{e^2}{2}\int_P \Delta^d(P)\left[N_F^-(P) + N_F^+(P)\right]\left(\frac{K^4}{(K\cdot P)^2} + \frac{2K^4k^0p^0}{(K\cdot P)^3} - \frac{K^6p_0^2}{(K\cdot P)^4}\right)$$

$$(\Pi^{\mathrm{Pow}})^{\mu}_{\mu} = \frac{e^2}{2}(D-2)\int_P \Delta^d(P)\left[N_F^-(P) + N_F^+(P)\right]\left[-\frac{K^4}{(K\cdot P)^2} + \frac{m^2K^6}{2(K\cdot P)^4}\right]$$

Calculations by (Endrődi and Markó, JHEP, 2022)

The second order term in the expansion of $\Pi_{00}^{T\neq 0}(0,k)$ around $k=0$ gives then the susceptibility, which reads (see the details again in App. A)

$$\left.\frac{\partial^2 \Re\, \Pi_{00}^{T\neq 0}(0,k)}{\partial k^2}\right|_{k=0} = -\frac{e^2}{3\pi^2}\int_m^\infty \frac{d\omega}{\sqrt{\omega^2-m^2}}\left(2n_F(\omega)-\omega\frac{dn_F(\omega)}{d\omega}\right), \tag{3.13}$$

and hence

$$\xi = -\frac{1}{6\pi^2}\int_m^\infty \frac{d\omega}{\sqrt{\omega^2-m^2}}\left(2n_F(\omega)-\omega\frac{dn_F(\omega)}{d\omega}\right). \tag{3.14}$$

One can expand in terms of m/T to obtain a high-temperature expansion (HTE) expression

$$\xi = -\frac{1}{12\pi^2}\left(\log\frac{T^2\pi^2}{m^2}-2\gamma_E+1\right)+\frac{31\zeta'(-4)}{192\pi^2}\frac{m^4}{T^4}+\mathcal{O}\left(\frac{m^6}{T^6}\right), \tag{3.15}$$

where $\zeta'(z)$ is the derivative of the Riemann ζ function. The leading term in (3.15) agrees with the results of Refs. [40, 49] for massless fermions – in that case m is replaced by the renormalization scale under the logarithm.

(Endrődi and Markó, PRD, 2024)

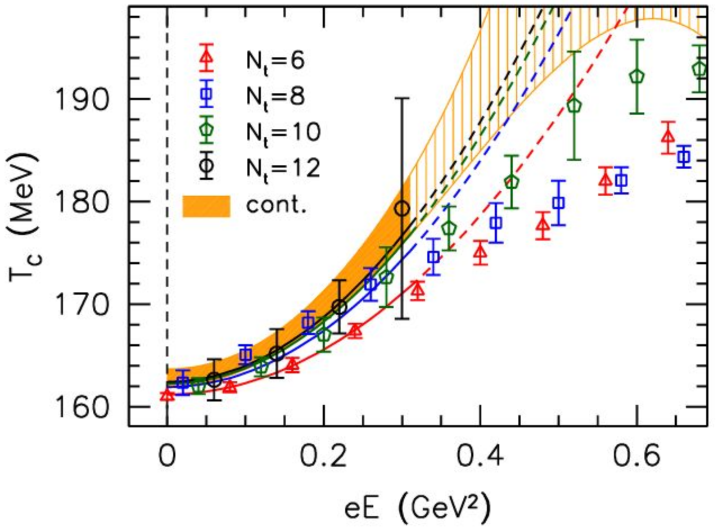

FIG. 3. Transition temperature as a function of the electric field for different lattice spacings (colored symbols) and a continuum extrapolation (yellow band). Higher-order effects in eE become non-negligible for $eE \gtrsim 0.3$ GeV^2, indicated by the dashed section of the fits.

Estimation of the electromagnetic field in intermediate-energy heavy-ion collision

Hidetoshi Taya,[1,*] Toru Nishimura,[2,3] and Akira Ohnishi[3]

[1] *RIKEN iTHEMS, RIKEN, Wako 351-0198, Japan*
[2] *Department of Physics, Osaka University, Toyonaka, Osaka, 560-0043, Japan*
[3] *Yukawa Institute for Theoretical Physics, Kyoto University, Kyoto, 606-8317, Japan*

We estimate the spacetime profile of the electromagnetic field in head-on heavy-ion collisions at intermediate collision energies $\sqrt{s_{\rm NN}} = \mathcal{O}(3\text{ - }10\ \text{GeV})$. Using a hadronic cascade model (JAM; Jet AA Microscopic transport model), we numerically demonstrate that the produced field has strength $eE = \mathcal{O}((30\text{ - }60\ \text{MeV})^2)$, which is supercritical to the Schwinger limit of QED and is non-negligibly large compared even to the hadron/QCD scale, and survives for a long time $\tau = \mathcal{O}(10\ \text{fm}/c)$ due to the baryon stopping. We show that the produced field is nonperturbatively strong in the sense that the nonperturbativity parameters (e.g., the Keldysh parameter) are sufficiently large, which is in contrast to high-energy collisions $\sqrt{s_{\rm NN}} \gtrsim 100$ GeV, where the field is merely perturbative. Our results imply that the electromagnetic field may have phenomenological impacts on hadronic/QCD processes in intermediate-energy heavy-ion collisions and that heavy-ion collisions can be used as a new tool to explore strong-field physics in the nonperturbative regime.